

# Depinning of Trapped Magnetic Flux in Bulk Niobium SRF Cavities

S. Aull\*

*CERN, Geneva, Switzerland and  
Universität Siegen, Germany*

J. Knobloch†

*Helmholtz-Zentrum Berlin, Germany and  
Universität Siegen, Germany*

(Dated: July 19, 2021)

Trapped magnetic flux is known to be a significant contribution to the residual resistance of superconducting radio frequency (SRF) cavities. The additional losses depend strongly if the vortices are depinned by the RF. The depinning is affected by the purity of the material, and the size of the pinning centers, as well as the cavity operation frequency. One may define a depinning frequency, above which significant depinning occurs. This publication presents a derivation of the depinning frequency from experimental data. We find a depinning frequency of 673 MHz for RRR 110 niobium. On this basis the currently used model is extended to describe the trapped flux sensitivity as function of residual resistance ratio (RRR) and operation frequency while also accounting for the pinning center size and the treatment history of the cavity. Moreover, the model offers an explanation for the significantly higher trapped flux sensitivity reported for nitrogen doped and 120° baked cavities.

PACS numbers: 29.20.-c , 74.25.N, 74.25.Wx

Keywords: flux pinning, trapped flux, residual resistance

## I. INTRODUCTION

Particle accelerators operating superconducting radio frequency (SRF) cavities in continuous wave (cw) mode or at high duty cycle require maximum quality factor rather than highest accelerating gradients. It is therefore mandatory to minimize any residual losses and hence trapped magnetic field which is one significant contributor to the residual resistance. While the BCS resistance decreases exponentially with temperature, the residual is temperature independent and becomes easily the dominant contribution at typical operation temperatures between 1.8 K and 2 K.

When an SRF cavity passes through the superconducting transition all ambient magnetic field should be expelled (Meissner effect). If no specific measures are taken, this expulsion is usually not complete and the magnetic flux is pinned at imperfections in the crystal lattice or impurities. These trapped vortices have a normal conducting core and dissipate power when oscillating under the influence of the RF field. Vallet and co-workers proposed a simple model to describe these additional losses due to trapped flux [19]:

$$R_{\text{TF}} = 3.6 \text{ n}\Omega/\mu\text{T} \sqrt{\frac{f}{\text{RRR}}} \quad (1)$$

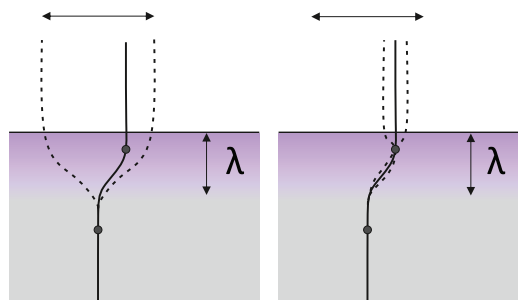


Figure 1. Flux line motion under the influence of an RF field. The solid line represents a single flux line trapped by two pinning centres. The dashed lines indicate the range of motion for the flux line assuming a bulk superconductor with  $f/f_0 \gg 1$  (left) and a bulk superconductor with  $f/f_0 \ll 1$  (right).

They consider the normal electrons in the core of a flux tube being lossy due to the skin effect which scales with the square root of the frequency  $f$  and with the square root of the electrical conductivity which in turn is inversely proportional to the residual resistance ratio  $\text{RRR}$ . The sensitivity of  $3.6 \text{ n}\Omega/\mu\text{T}$  was derived experimentally using a 1.5 GHz cavity made from RRR 300 material. This simple model holds however only if the trapped vortices actually move under the influence of the RF field.

The displacement of a single flux line can be described as a damped oscillator accounting for the Lorentz force due to a transport current  $J_{\text{T}}$ , the frictional force and the pinning force [8, 9, 15]:

\* sarah.aull@cern.ch

† jens.knobloch@helmholtz-berlin.de

$$m\ddot{x} + \eta\dot{x} + kx = \frac{J_T\Phi_0}{c} \quad (2)$$

Here  $m$  is the effective mass of the vortex. The contribution from this term can be neglected as the RF period ( $> 10^{-8}$  s) is much larger than the relaxation time of a vortex  $\tau \sim m$ , which was estimated by H. Suhl to be in the order of  $10^{-12}$  s [15, 17].  $k$  accounts for the pinning force and depends on the size, geometry and type of the pinning centre.

The flux flow viscosity  $\eta$  is given by the flux quantum  $\Phi_0$  divided by the squared speed of light  $c^2$ , the upper critical field  $H_{c2}$  and the electrical resistivity  $\rho_n$  [16]:

$$\eta = \frac{\Phi_0 H_{c2}}{c^2 \rho_n}. \quad (3)$$

The depinning frequency  $f_0$  is defined as the frequency where 50% of the pinned vortices are depinned and is given by the ratio of pinning constant and flux flow viscosity [14]:

$$f_0 = \frac{k}{\eta} \quad (4)$$

If the RF frequency is well above the depinning frequency, the majority of trapped vortices are depinned. However, if the superconductor is thicker than the penetration depth  $\lambda$ , as it is the case for SRF cavities, the trapped vortices are only depinned in the RF layer and stay pinned in the bulk. They are then oscillating within the RF layer but cannot move entirely freely or be expelled from the material. This scenario is depicted in Fig. 1 on the left. If the RF frequency is well below the depinning frequency, the pinning is effective and the flux line can only move in between pinning centers as indicated in Fig. 1 on the right. Based on Gittleman and Rosenblum's calculation of the impedance of samples thinner than the penetration depth [9], we define a depinning efficiency for bulk superconductors to describe how many flux lines are depinned depending on the ratio of RF frequency to depinning frequency and plot it in Figure 2:

$$\varepsilon_{\text{depin}} = \frac{f^2}{f^2 + f_0^2} \quad (5)$$

Since  $\rho_n$  is inversely proportional to the conductivity and therefore to the RRR, the depinning frequency scales with  $1/RRR$ . Considering typical SRF cavities, we can then identify two distinct regimes in Fig. 2: A lower regime where  $f/f_0 \ll 1$  so that pinning is very efficient and the upper part where  $f/f_0 \gg 1$  so that all flux lines are depinned. The first can be obtained by the combination of low RF frequency and low RRR (=

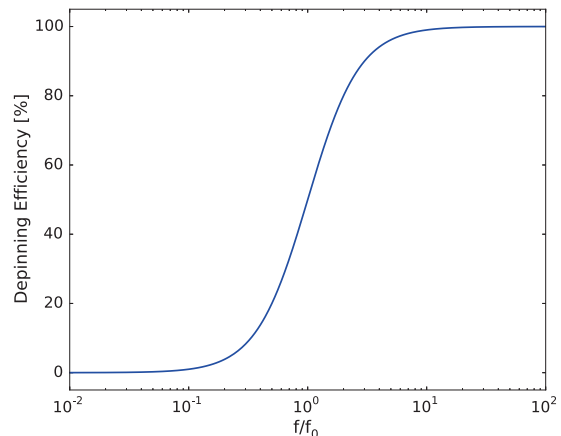


Figure 2. Depinning efficiency as function of the ratio between operating and depinning frequency. For  $f/f_0 \gg 1$  all flux lines are depinned while for  $f/f_0 \ll 1$  all flux lines are pinned and do not dissipate power.

large  $f_0$ ) as typical for niobium coated cavities. The latter represents the combination of high RF frequency and high RRR (=low  $f_0$ ) as typical for bulk niobium cavities. This could already explain why niobium coated cavities are at least one to two orders of magnitude less sensitive to trapped flux as bulk [4, 23] so that they do not require magnetic shielding [5].

## II. DEPINNING FREQUENCY

Bulk niobium cavities are nowadays made from high RRR ( $> 250$ ) niobium and are designed for rather high operation frequencies ( $> 1$  GHz). This combination usually places the cavities on the upper plateau of the depinning curve in Fig. 2. Arnolds-Mayer and Chiaveri published in 1987 trapped flux measurements on a 500 MHz cavity of RRR 110 material [1]. The authors derive a trapped flux sensitivity of  $1.22 \text{ n}\Omega/\mu\text{T}$ . Following Eq. 1 as proposed by Vallet and co-workers, a trapped flux sensitivity of  $3.4 \text{ n}\Omega/\mu\text{T}$  would be expected. Comparing the measurement of Arnolds-Mayer and Chiaveri with the prediction of Vallet et. al. yields a depinning efficiency of 35.5% placing this measurement on the slope between the pinning and depinning regime. Equation 5 can now be used to calculate the depinning frequency for RRR 110:

$$f_0 = \sqrt{\frac{f^2 (\varepsilon_{\text{pin}} - 1)}{\varepsilon_{\text{pin}}}} = 673 \text{ MHz} \quad (6)$$

For other RRR values the depinning frequency can be scaled via  $1/RRR$ . Figure 3 displays the change of  $f_0$  with RRR. As can be seen, the depinning frequency increases dramatically for low RRR values. For niobium

films a RRR of 10 to 20 is typical. The depinning frequency for this range is between 3.7 GHz and 7.4 GHz. This is consistent with niobium film cavities being almost insensitive to trapped flux even at 1.5 GHz [4]. In contrast to the niobium films, the depinning frequency for RRR 300 is 247 MHz.

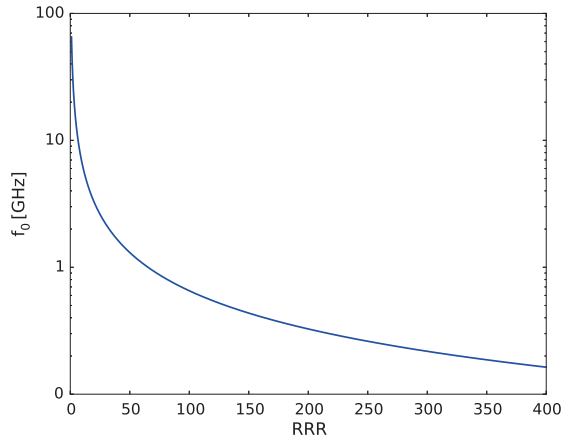


Figure 3. Depinning frequency as function of RRR.

### III. TRAPPED FLUX SENSITIVITY

In order to describe additional residual resistance due to trapped flux, we account for three aspects: The losses of depinned vortices under the influence of the RF field, the percentage of vortices that get depinned and the total

$$S_{\text{TF}} = 3.6 \text{ n}\Omega/\mu\text{T} \sqrt{\frac{f}{1.5 \text{ GHz}} \frac{300}{\text{RRR}}} \cdot \frac{f^2}{f^2 + \left(p \cdot 673 \text{ MHz} \frac{110}{\text{RRR}}\right)^2} \cdot \varepsilon_{\text{trap}} \quad (7)$$

The effect of the treatment history and the base material (large grain vs fine grain) are described by a trapping efficiency  $\varepsilon_{\text{trap}}$  and can be taken from [2] for several material and treatment combinations. Folding these three aspects into a trapped flux sensitivity results in Eq. 7 which can be tested against SRF measurements. The corresponding total increase of residual resistance due to trapped flux is then  $R_{\text{TF}} = S_{\text{TF}} \cdot B_{\text{app}}$ .

Table I lists available trapped flux measurements where the effect of cooling can be neglected and sufficient information about the treatment and the cavity material is reported. Depending on the treatment, a flux trapping efficiency  $\varepsilon_{\text{trap}}$  is assumed based on [2] and listed in Tab. I. It can be seen that Eq. 7 agrees well with the available cavity data for medium and high RRR values. The effect of RRR, frequency and relative pinning center size on the

amount of trapped field in the material. The first factor is well described by Vallet and co-workers with dependency on frequency and RRR according to the normal skin effect. The second factor is given by the depinning efficiency as described in Eq. 5 and the depinning frequency can be scaled from Eq. 6. However, not only the RRR defines the depinning frequency but also the size of the pinning center. Larkin and Ovchinnikov [12] discuss pinning of a single vortex parallel to a grain boundary. They conclude that the depinning frequency increases linearly with the thickness of the grain boundary. Flux trapping measurements on bulk niobium samples suggest that grain boundaries are the most severe pinning centers in cavity material [2]. Based on Larkin and Ovchinnikovs calculations, we introduce a relative pinning center size  $p$  which is normalized to standard high quality bulk niobium as nowadays used for SRF cavities.

Lastly, the amount of trapped flux has to be estimated. It has been shown that the residual resistance increases linearly with the applied (dc) magnetic field  $B_{\text{app}}$  up to 6 times the earth magnetic field strength [2, 20]. However, the treatment history and the crystal structure of the material has an influence on how much of the ambient field actually gets trapped [2]. Moreover, recent studies show that acting on the cool down dynamics at the superconducting transition can lead to improved flux expulsion [2, 13, 21]. In the following, we will restrict the discussions to trapped flux measurements where the additional residual resistance due to trapped flux is high enough so that cool down effects can be neglected. Moreover, we restrict ourselves to cavity measurement cooled down in an axial field since it has been recently shown that the direction of the field has also an influence on the trapped flux sensitivity [6].

trapped flux sensitivity will be subject in the following sections.

#### A. The Influence of RRR

Figure 4 shows the trapped flux sensitivity for different cavity frequencies as function of RRR. For high RRR values and low frequency the trapped flux sensitivity is basically constant. For high frequencies however, there is slight decrease with increasing RRR. The measurements on large grain niobium reported in [7] list a RRR of 200 before baking. It can be expected that the baking at 1250 °C increased the RRR due to the post-purification process [7]. The prediction can be brought to agreement with the measurement for a RRR value of 320 which ap-

Table I. Measured trapped flux sensitivity for different bulk Nb cavities. The measurements are compared with the calculation according to Eq. 7. Frequency and RRR are taken from the references. If the mean free path  $\ell$  is given, the RRR was calculated as  $\ell[\text{nm}] = 2.7 \cdot \text{RRR}$ . The relative pinning center size  $p$  was set to 1 for all listed calculations. See text for discussion on  $p$  for the N doped and  $120^\circ$  baked cavities.

	RRR	Frequency [GHz]	meas. trapped flux sensitivity [nΩ/μT]	calc. trapped flux sensitivity [nΩ/μT]	$\epsilon_{\text{trap}}$	Ref.
Cavity	300	1.5	3.6	3.5	100 %	[19]
Cavity	110	0.5	1.22	1.22	100 %	[1]
Large grain cavity + BCP	200	1.5	$2.5 \pm 0.2$	3.0	73 %	[7]
Large grain cavity + 1250 °C + BCP	200	1.5	$1.43 \pm 0.12$	1.75	42 %	[7]
N doped cavity	3.3	1.3	11.3	0.1 <sup>a</sup>	100 %	[10]
120° baked cavity	8.5	1.3	3.7	0.4 <sup>b</sup>	100 %	[10]

<sup>a</sup> The calculation can be brought to an agreement with the measurement for  $p = 0.08$ . See text for discussion.

<sup>b</sup> The calculation can be brought to an agreement with the measurement for  $p = 0.31$ . See text for discussion.

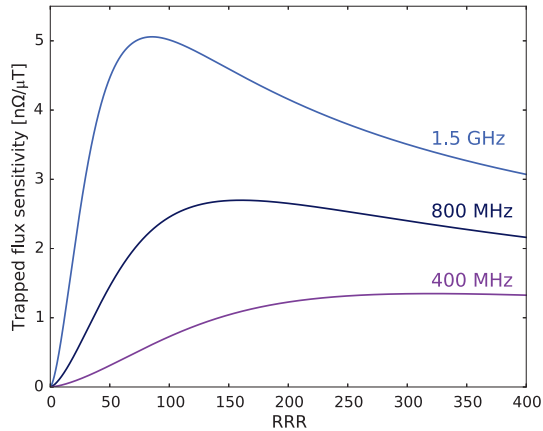


Figure 4. Trapped flux sensitivity as function of RRR for different frequencies.

pears plausible. Moreover, Fig. 4 reveals an increase of trapped flux sensitivity when going from high RRR to intermediate values and a rapid decrease for very low RRR values. The very strong change in trapped flux sensitivity for low RRR values, especially at high frequency requires therefore information about the surface RRR to make a reliable prediction.

It should also be noted that the scaling with  $\sqrt{f/\text{RRR}}$  for the losses as described by Eq. 1 are based on the normal skin effect. For high RRR values the mean free path becomes comparable to the skin depth and the anomalous skin effect has to be applied. In this regime, the losses in the normal conducting core become independent of the RRR and scale with  $f^{2/3}$ .

## B. The Influence of the Pinning Center Size

Figures 5 and 6 plot the trapped flux sensitivity as function of the relative pinning center size  $p$  for 400 MHz

and 1.3 GHz. The trend for both frequencies is very similar: for high RRR the trapped flux sensitivity depends only slightly on the pinning center size. The dependency however becomes stronger the shorter the mean free path gets and the effect is more emphasized for high frequencies.

There are several trapped flux measurements at 1.3 GHz with a base material of RRR 300 which were baked at  $120^\circ$  or nitrogen doped [10]. Both treatments result in a drastic reduction of surface RRR. The measured trapped flux sensitivity of both cavities is significantly higher compared to what would be expected from either Eq. 1 or Eq. 7. Recent findings suggest that the  $120^\circ$  baking as well as the nitrogen doping reduces or even prohibits the formation of nanohydrides which most likely act as pinning centers [18, 22]. Moreover, it is suggested that the size of the nanohydrides is reduced. Assuming nanohydrides to be pinning centers, our model supports a reduced pinning center size: An agreement with the measurements can be obtained for a relative pinning center size of 0.08 for the N doping and 0.31 for the  $120^\circ$  baking.

The relative pinning center size can also be estimated from measurements with the Quadrupole Resonator which allows measurements of the surface resistance for 400 MHz, 800 MHz and 1200 MHz with the same field configuration. The full description of the set-up, the measurement method and parameter range can be found elsewhere [11]. Recent upgrades allow applying a dc magnetic field to the sample under test. The field strength is measured with a cryogenic magnetic field probe (Mag-01H [3]). In a dedicated test, a reactor grade bulk Nb sample with RRR 47 was cooled down in different ambient fields and the surface resistance was measured at 2.5 K and low RF field ( $\approx 10$  mT). For each trapped field, the surface resistance was measured at each of the three resonant frequencies (400 MHz, 800 MHz and 1200 MHz). In this way, the trapped flux sensitivity was derived as function of frequency and is plotted in Fig. 7. The relative pinning center size can now be fitted using Eq. 7. We find excellent agreement for  $p = (2.8 \pm 0.1)$ . The rel-

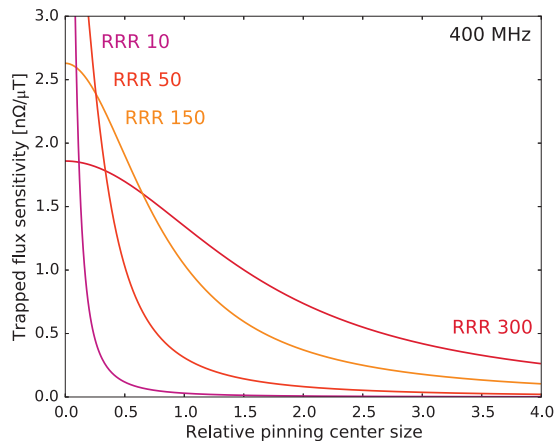


Figure 5. Trapped flux sensitivity as function of pinning center size for 400 MHz.

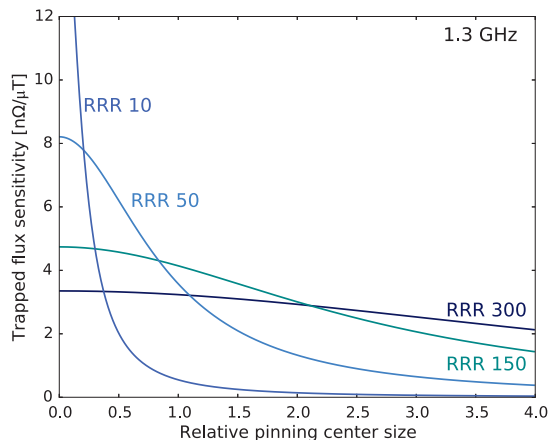


Figure 6. Trapped flux sensitivity as function of pinning center size for 1.3 GHz.

atively bigger pinning center size for this sample appears plausible as the base material is reactor grade niobium. This is in contrast to measurements on cavities where the base material was of high quality and the mean free path was shortened due to diffusion processes of dissolved gases upon baking. Our measurement supports therefore the validity of Eq. 7 and the assumptions made.

#### IV. SUMMARY AND CONCLUSION

Depinning of trapped vortices has to be considered when predictions for the trapped flux sensitivity of SRF

cavities should be made. The depinning efficiency depends on the size of the pinning centers and the RF frequency. Trapped flux measurements on a low frequency and medium RRR cavity allowed deriving the according

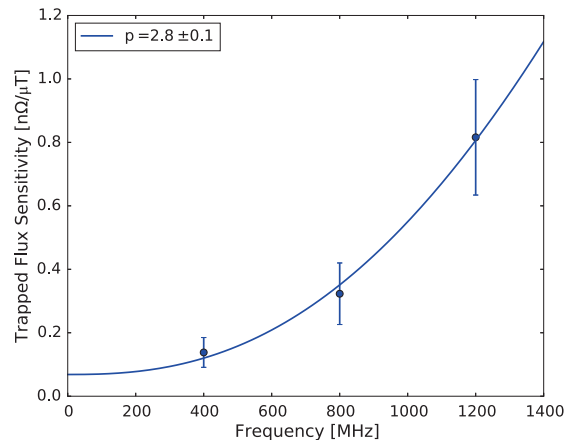


Figure 7. Trapped flux sensitivity measured with the Quadrupole Resonator for 400 MHz, 800 MHz and 1200 MHz of a RRR 47 bulk Nb sample.

depinning frequency which can be scaled to other RRR values. On this basis we propose an extended model for describing the additional losses due to trapped flux. To date, only the losses in the normal core due to the skin effect have been taken into account. We account additionally for depinning which depends on the RRR, operation frequency and the pinning center size as well as for the trapping efficiency. The predictions made are in good agreement with our measurements and measurements done at other labs covering a variety of frequency, RRR and treatment combinations. Moreover, the model offers an explanation why cavities with short mean free path are much more sensitive to trapped flux than the simple model suggests.

#### ACKNOWLEDGMENTS

We would like to acknowledge V. Palmieri for calling our attention to the publications on depinning. We thank W. Venturini Delsolaro and T. Junginger for fruitful discussions and help with the Quadrupole Resonator. Moreover, we thank J. Bremer, L. Dufay-Chanat and T. Koettig for providing the cryogenic infrastructure and technical help, as well as G. Pechaud and S. Forel for preparing the sample for the tests in the Quadrupole Resonator. This work is sponsored by the Wolfgang Gentner Programme of the German Federal Ministry of Education and Research (BMBF).



- 
- [1] G. Arnolds-Mayer and E. Chiaveri. On a 500 MHz Single Cell Cavity with Nb<sub>3</sub>Sn Surface. In *Proceedings of the 3rd Workshop on RF Superconductivity*, Argonne, USA, 1987. URL: <http://epaper.kek.jp/srf87/papers/srf87e03.pdf>.
- [2] S. Aull, O. Kugeler, and J. Knobloch. Trapped magnetic flux in superconducting niobium samples. *Physical Review Special Topics - Accelerators and Beams*, 15(6), June 2012. URL: <http://link.aps.org/doi/10.1103/PhysRevSTAB.15.062001>, doi:10.1103/PhysRevSTAB.15.062001.
- [3] Mag-01 & Mag-01h - Single Axis Fluxgate Magnetometers, 2014. [www.bartington.com](http://www.bartington.com).
- [4] C. Benvenuti, S. Calatroni, I. E. Campisi, P. Darriulat, M. A. Peck, R. Russo, and A.-M. Valente. Study of the surface resistance of superconducting niobium films at 1.5 GHz. *Physica C: Superconductivity*, 316(3):153–188, 1999. URL: <http://www.sciencedirect.com/science/article/pii/S0921453499002075>, doi:[http://dx.doi.org/10.1016/S0921-4534\(99\)00207-5](http://dx.doi.org/10.1016/S0921-4534(99)00207-5).
- [5] Brüning, O., Poole, J., Collier, P., Lebrun, P., Ostojic, R., Myers, S., and Proudlock, P. The LHC Main Ring. *LHC Design Report*, I:548, 2004. URL: <http://dx.doi.org/10.5170/CERN-2004-003-V-1>, doi:10.5170/CERN-2004-003-V-1.
- [6] M. Checchin, M. Martinello, A. Grassellino, O. Melnychuk, A. Romanenko, and D. A. Sergatskov. Origin of the trapped flux caused by quench in superconducting niobium cavities. In *Proceedings of the 6th International Particle Accelerator Conference*, page 3, 2015. URL: <https://jacowfs.jlab.org/conf/proceedings/IPAC2015/papers/wepty021.pdf>.
- [7] G. Ciovati and A. Gurevich. Measurement of RF Losses due to Trapped Flux in Large-Grain Niobium Cavity. In *Proceedings of the 13th Workshop on RF Superconductivity*, pages 132–136, Peking, China, 2007. URL: <http://accelconf.web.cern.ch/AccelConf/srf2007/PAPERS/TUP13.pdf>.
- [8] J. I. Gittleman and B. Rosenblum. Radio-Frequency Resistance in the Mixed State for Subcritical Currents. *Physical Review Letters*, 16(17):734–736, April 1966. URL: <http://link.aps.org/doi/10.1103/PhysRevLett.16.734>, doi:10.1103/PhysRevLett.16.734.
- [9] J. I. Gittleman and B. Rosenblum. The Pinning Potential and High-Frequency Studies of Type-II Superconductors. *Journal of Applied Physics*, 39(6):2617, 1968. URL: <http://scitation.aip.org/content/aip/journal/jap/39/6/10.1063/1.1656632>, doi:10.1063/1.1656632.
- [10] D. Gonella and M. Liepe. Flux trapping in nitrogen-doped and 120c baked cavities. In *Proceedings of the 5th International Particle Accelerator Conference*, page 3, Dresden, Germany, June 2014. JACoW. URL: <http://accelconf.web.cern.ch/AccelConf/IPAC2014/>.
- [11] T. Junginger, W. Weingarten, and C. Welsch. Extension of the measurement capabilities of the quadrupole resonator. *Review of Scientific Instruments*, 83:063902, 2012. URL: <http://dx.doi.org/10.1063/1.4725521>, doi:10.1063/1.4725521.
- [12] A. I. Larkin and Yu. N. Ovchinnikov. Pinning in type II superconductors. *Journal of Low Temperature Physics*, 34(3-4):409–428, February 1979. URL: <http://link.springer.com/10.1007/BF00117160>, doi:10.1007/BF00117160.
- [13] A. Romanenko, A. Grassellino, O. Melnychuk, and D. A. Sergatskov. Dependence of the residual surface resistance of superconducting radio frequency cavities on the cooling dynamics around T<sub>c</sub>. *Journal of Applied Physics*, 115(18):184903, May 2014. URL: <http://scitation.aip.org/content/aip/journal/jap/115/18/10.1063/1.4875655>, doi:10.1063/1.4875655.
- [14] A. Schmid and W. Hauger. On the theory of vortex motion in an inhomogeneous superconducting film. *Journal of Low Temperature Physics*, 11(5-6):667–685, June 1973. URL: <http://link.springer.com/10.1007/BF00654452>, doi:10.1007/BF00654452.
- [15] Y. Shapira and L. J. Neuringer. Magnetoacoustic Attenuation in High-Field Superconductors. *Physical Review*, 154(2):375–385, February 1967. URL: <http://link.aps.org/doi/10.1103/PhysRev.154.375>, doi:10.1103/PhysRev.154.375.
- [16] A. R. Strnad, C. F. Hempstead, and Y. B. Kim. Dissipative Mechanism in Type-II Superconductors. *Physical Review Letters*, 13(26):794–797, December 1964. URL: <http://link.aps.org/doi/10.1103/PhysRevLett.13.794>, doi:10.1103/PhysRevLett.13.794.
- [17] H. Suhl. Inertial Mass of a Moving Fluxoid. *Physical Review Letters*, 14(7):226–229, February 1965. URL: <http://link.aps.org/doi/10.1103/PhysRevLett.14.226>, doi:10.1103/PhysRevLett.14.226.
- [18] Y. Trenikhina, A. Romanenko, J. Kwon, J.-M. Zuo, and J. F. Zasadzinski. Nanostructural features affecting superconducting radio frequency niobium cavities revealed using TEM and EELS. *arXiv preprint arXiv:1503.02046*, 2015. URL: <http://arxiv.org/abs/1503.02046>.
- [19] C. Vallet, M. Bolor, and B. Bonin. Residual RF Surface Resistance Due to Trapped Magnetic Flux. Technical Report 93 15, DAPNIA/CE Saclay, September 1993.
- [20] C. Vallet, M. Bolor, B. Bonin, J. P. Charrier, B. Daillant, J. Gratadour, F. Koechlin, and H. Safa. Flux Trapping in Superconducting Cavities. In *Proceedings of the 3rd European Particle Accelerator Conference*, pages 1295–1297, Berlin, Germany, 1992. URL: [http://accelconf.web.cern.ch/AccelConf/e92/PDF/EPAC1992\\_1295.PDF](http://accelconf.web.cern.ch/AccelConf/e92/PDF/EPAC1992_1295.PDF).
- [21] J.-M. Vogt, O. Kugeler, and J. Knobloch. Impact of cool-down conditions at T<sub>c</sub> on the superconducting rf cavity quality factor. *Physical Review Special Topics - Accelerators and Beams*, 16(10), October 2013. URL: <http://link.aps.org/doi/10.1103/PhysRevSTAB.16.102002>, doi:10.1103/PhysRevSTAB.16.102002.
- [22] Y. Trenikhina. TEM studies of cavity cutouts form EP niobium SRF cavities prepared by different treatments, July 2014.
- [23] P. Zhang. The Influence of Cooldown Conditions at Transition Temperature on the Quality Factor of Niobium Sputtered Quarter-Wave Resonators, August 2014. URL: <http://www.surfacetreatments.it/thinfilms-2014/index.asp>.